

Evolution of Neurofilament Subtype Accumulation in Axons Following Diffuse Brain Injury in the Pig

XIAO-HAN CHEN, MD, DAVID F. MEANEY, PhD, BAI-NAN XU, MD, MASAHIRO NONAKA, MD, TRACY K. MCINTOSH, PhD, JOHN A. WOLF, KATHRYN E. SAATMAN, PhD, AND DOUGLAS H. SMITH, MD

Abstract. Although accumulation of neurofilament (NF) proteins in axons has been recognized as a prominent feature of brain trauma, the temporal course of the accumulation of specific NF subtypes has not been well established. In the present study, 17 miniature swine were subjected to nonimpact inertial brain injury. At 3 hours (h), 6 h, 24 h, 3 days, 7 days, and 10 days post-trauma, immunohistochemical analysis was performed to determine axonal accumulation of NF-light (NF-L), the rod and sidearm domains and sidearm phosphorylation states of NF-medium (NF-M), and heavy (NF-H). We found that NF-L accumulation was easily identified in damaged axons by 6 h post-trauma, but NF-M and H accumulation was not clearly visualized until 3 days following injury. In addition, the axonal accumulation of NF-M and H appeared to be primarily comprised of the sidearm domains. While the accumulating NF was found to be predominantly dephosphorylated, we also detected accumulation of phosphorylated NF. Finally, we found that developing axonal pathology may proceed either towards axotomy with discrete terminal bulb formation or towards the development of varicose swellings encompassing long portions of axons. These findings suggest that there is a differential temporal course in NF subtype disassembly, dephosphorylation, and accumulation in axons following initial brain trauma and that these processes occur in morphologically distinct phenotypes of maturing axonal pathology.

Key Words: Diffuse axonal injury; Inertial brain injury; Neurofilament; Phosphorylation.

INTRODUCTION

Diffuse axonal injury (DAI) is commonly observed following brain trauma and is a primary cause of death and neurological disability (1–4). While multiple studies have established that accumulation of the structural neurofilament (NF) proteins are key features of DAI (5–10), little is known regarding the temporal evolution of NF subtype accumulation following brain trauma.

NF proteins are primary cytoskeleton components of axons, neuronal soma, and dendrites and consist of 3 related polymeric proteins of 68, 150 and 200 KD, respectively referred to as neurofilament light (NF-L), medium (NF-M), and heavy (NF-H). While each subtype of NF protein is composed of similar rod domains, the structure of NF-M and H also include sidearm domains of differing lengths and the extent of sidearm phosphorylation is thought to influence the diameter of axons (11–13). It has been proposed by Povlishock and others that trauma induces compaction of NF due to proteolysis of the sidearm domains resulting in impaired transport (axoplasmic flow) and subsequent swelling (14, 15). Further disorganization of the axonal cytoskeleton and organelle accumulations are thought to lead to the disconnection of axon with the signature pathologic feature of a bulb formation at the terminal end of the axon. While it is thought that all disconnected axons ultimately undergo Wallerian degeneration,

alternate pathways of secondary or delayed axonal damage following trauma have not been fully explored.

In the present study, we utilized immunohistochemical techniques to evaluate the disposition of NF subtype proteins in damaged axons following diffuse brain injury in the pig. In addition, we evaluated the development of different morphologies or “phenotypes” of developing axonal pathology following trauma. The most salient feature of this model of diffuse brain injury in the pig is the production of widespread axonal pathology in the white matter resulting from nonimpact rotational acceleration of the head as previously reported (16). This head rotation induces inertial loading to the pig brain that is representative of the loading conditions that often occurs to human brains during traumatic events such as automotive crashes. Pigs were selected because of their relatively large gyrencephalic brains with substantial white matter domains and for their proven ability to develop diffuse axonal injury similar to the human condition (16).

MATERIALS AND METHODS

In these studies, we carefully adhered to the animal welfare guidelines set forth in the *Guide for the Care and Use of Laboratory Animals*, U.S. Department of Health and Human Services Publication, 85-23. All animal procedures were approved by the University of Pennsylvania Institutional Animal Care and Use Committee.

Preinjury Preparation

Nineteen miniature young adult swine (n = 17 injured and n = 2 normal control), (4 months of age, Hanford and Hormel strains), both male and female, weighing 17–

From the Departments of Neurosurgery (X-HC, B-NX, MN, TKM, JAW, KES, DHS) and Bioengineering (DFM), University of Pennsylvania School of Medicine, Philadelphia, Pennsylvania.

Correspondence to: Douglas H. Smith, MD, Department of Neurosurgery, University of Pennsylvania School of Medicine, 105 Hayden Hall, 3320 Smith Walk, Philadelphia, PA 19104-6316.

This study was funded, in part, by grants NS38104, AG12527, NS08803, and a grant from the Whitaker Foundation.

20 kg, were used for this study. The animals were fasted for 12 h, whereupon anesthesia was induced with an initial injection of midazolam (400–600 mg/kg). Once sedated, the animals received 2–4% isoflurane via snout mask until they reached a plane of surgical anesthesia. A venous catheter was then inserted in the ear, and the animals were endotracheally intubated and maintained on 1.5–2% isoflurane. Physiologic monitoring and apparatus included noninvasive ECG electrode leads affixed to the chest and extremities, a pulse oximeter placed on the skin of the tail, a rectal thermometer, and sampling tubes for end tidal CO₂ measurement attached to the endotracheal tube. Arterial blood gasses were also periodically evaluated prior to injury and following injury. The pigs were continuously monitored and all data from physiologic monitoring were collected on a computer driven storage system. Intracranial pressure monitoring was not performed since previous studies demonstrated only small transient changes with the injury parameters applied in this study (16).

Brain Injury

Brain trauma was induced via head rotational acceleration as previously described in detail (16). Briefly, the animals' heads were secured to a padded snout clamp, which in turn is mounted to the linkage assembly of a pneumatic actuator device that converts the linear motion to an angular (rotational) motion. For these experiments, the linkage was adjusted to produce a pure impulsive head rotation in the coronal plane, with the center of rotation close to the brain center of mass. Isoflurane anesthesia was withdrawn 10 s prior to injury. Head rotational acceleration was biphasic with a predominant deceleration phase. Triggered release of pressurized nitrogen rotated the linkage assembly 110° in 20 ms. Following injury, the animals' heads were released from the device. All animals received buprenorphine (0.1mg/kg, i.m., q12h, p.r.n.) for postoperative analgesia. It is important to note that previous studies with these techniques demonstrated injured animals were awake and ambulatory within 8 hours (h) of injury (16).

Tissue Preparation

At selected time points following brain injury (n = 3 at 3 h, n = 3 at 6 h, n = 2 at 1 day, n = 3 at 3 days, n = 4 at 7 days, n = 2 at 10 days, n = 2 normal control) animals were euthanized by overdose injection of pentobarbital (150 mg/kg I.V.) and transcardially perfused with saline followed by 4% paraformaldehyde. The brains were removed and postfixed in 4% paraformaldehyde and stored in phosphate buffer solution and cryoprotected with sucrose. Subsequently, the brains were blocked into 0.5-cm coronal sections for gross examination and photography. A series of 40- μ m-frozen sections

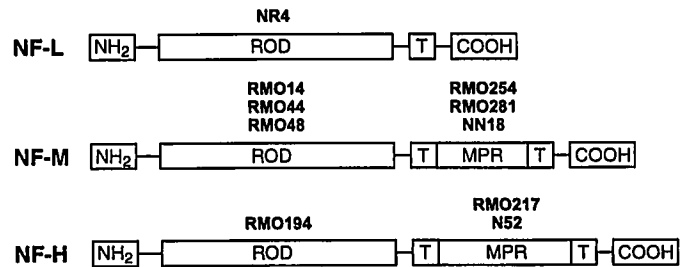


Fig. 1. Schematic representation of the structure of NF subtype proteins and the antigenic epitopes of the primary antibodies employed in this study. All 3 NF proteins are made up of a highly conserved 'rod' domain at the amino terminus, and NF-M and H also have a sidearm domain at the carboxy terminal 'tail' (T) that includes a multiphosphorylation region (MPR). While antibody NR4 does not have a characterized binding site on NF-L, RMO14, RMO44, RMO48, and RMO194 antibodies specifically recognize epitopes on the rod domain of NFM and NFH. Antibodies NN18, RMO281, and RMO217 are specific for phosphorylation-dependent epitopes on the NF-M and H sidearms. Antibodies N52 and RMO254 are specific for nonphosphorylated NF-M and H sidearms.

were cut from the front face of each block and 10 parallel sets saved for immunohistochemistry.

Immunohistochemistry and Analysis

Neurofilament immunohistochemistry was performed on free flotation sections using the avidin-biotin-peroxidase complex (ABC) method (Vector Labs, Ingold, CA). Multiple primary monoclonal antibodies were used to elucidate NF subtype accumulation following trauma, shown in Figure 1. These antibodies included NR4 antibody, targeting the 68 KD NF subunit (Sigma, 1:400), NN18 antibody, to the phosphorylated 160 KD NF sidearm domains (Sigma 1:40), and N52 antibody, targeting the phosphorylation-independent 200 KD NF sidearm domains (Sigma, 1:400). RMO254 antibody, targeting phosphorylation-independent NF-M sidearms to C-terminus (Dr. V.M.-Y. Lee 1:5). RMO217 antibody, targeting phosphorylated NF-H sidearms to C-terminus (Dr. V.M.-Y. Lee 1:5 (17)). RMO281 antibody, targeting phosphorylated NF-M sidearms to C-terminus (Dr. V.M.-Y. Lee 1:5) (14). RMO14, RMO44, RMO48 antibodies, specific to recognize the rod domains of the NF-M subunit (Dr. V.M.-Y. Lee 1:500). RMO194 antibody, specific to recognize the rod domains of the NF-H subunit (Dr. V.M.-Y. Lee 1:500) (18) (Fig. 1). The sections were incubated with primary antibody overnight at 4°C and then incubated at room temperature for 1 h, each with the appropriate secondary antibodies and ABC solution (1:1,000). Antibodies were diluted in 0.1 M Tris buffer with 2% horse serum, and tissue sections were washed in this serum buffer. Peroxidase activity was revealed with 0.025% 3,3'-diaminobenzidine, 300 mg Imidazole and 0.25% H₂O₂ for 10 min. Omission of primary antibody or application of control serum in lieu of primary antibody on

selected sections of pig tissue provided a negative control.

Light microscopy was performed using a Nikon Microphot SA with UFX-DX camera system (Optical Apparatus, Ardmore, PA). Coronal sections representing the rostral-caudal extent of each brain were examined, and a semiquantitative analysis was performed to determine the number of axonal pathology profiles elucidated by each stain, as previously described (16). For overall axonal pathology, we used a sector scoring method to map out the approximate amount and distribution of axonal pathology. Regional axonal injury severity was determined according to the scheme: 1+ = 1–5 profiles/1.2 mm², 2+ = 6–15 profiles/1.2 mm², 3+ = >15 profiles/1.2 mm². To evaluate neurofilament subtype accumulation in axons, we selected sections from the cerebral peduncle and from white matter of frontal lobe (regions with a high density of axonal bulbs and axonal swelling). Four consecutive fields were counted for each staining.

RESULTS

Temporal Course of NF Subtype Accumulation in Damaged Axons after Brain Injury

In control animals, no axonal damage was found with any of the NF immunostains. In brain injured animals, no NF accumulation in damaged axons was detected by any of the NF antibodies at 3 h postinjury, but by 6 h postinjury, NF-L immunoreactivity revealed axonal swellings in the subcortical white matter of frontal and parietal lobes as well as brain stem (Fig. 2). These swellings appeared tortuous with multiple varicosities, but no axotomy was observed. By 24 h postinjury, NF-L immunostaining revealed a much greater number of axonal swellings; many of which had large diameters of greater than 10 μ m. In addition, at 24 h postinjury, NF-L immunostaining revealed frank disconnection at the distal portion of some axons with the classic bulb or terminal club formation due to terminal swelling. In contrast, none of the immunostains for NF-M or H revealed axonal pathology at 3 h or 6 h post-trauma and by 24 h only faint axonal staining suggestive of swellings could be discerned with these stains. However, by 3 days postinjury, axonal pathology was clearly and consistently elucidated with NF-M and H immunostains (Fig. 2). A high density of axonal swellings and bulbs were found in the deep white matter at the root of the gyri and at the junction of white and gray matter in the frontal, parietal, temporal, and occipital lobes. In addition, axonal injury was also observed at the margin of lateral ventricles external capsule, thalamus, cerebellum, and brainstem. This pattern was also found with NF-L immunostaining at 3 days following injury and remained consistent for NF-L, M and H subtypes at both 7 and 10 days post-trauma. Although there were modest differences in the apparent severity

and distribution of axonal pathology between animals in each group, the temporal differences found in NF subtype staining were completely consistent in all animals from each group. The severity and distribution of axonal pathology at 3 to 10 days post-trauma is consistent with that previously found at 7 days postinjury (16).

Axonal Accumulation of NF-M and H Rod and Sidearm Domains and Phosphorylation States

Antibodies to the NF rod domains (RMO14, RMO44, RMO48, and RMO194) showed no evidence of axonal immunoreactivity at any timepoint postinjury (Fig. 3). However, these antibodies stained neuronal soma consistent with previous reports (14, 18). This immunoreactivity in neuronal soma is used as a positive internal control to demonstrate the sensitivity of the antibodies. It has been suggested that since NF-M and H in the somata lack the highly phosphorylated sidearms, antibodies targeting the "core" rod domains have greater access to immunoreactive binding sites (18).

Using the antibodies specific for phosphorylation-independent NF-M and H sidearm domains (N52, RMO254), axonal pathology was readily identified in the deep white matter, gray matter, and brainstem. Antibodies specific for phosphorylated NF-M and H sidearm domains (NN18, RMO217, and RMO281) also revealed axonal pathology in a similar distribution. However, axonal pathology appeared to be much less dense and the staining was substantially weaker with phosphorylation-dependent antibodies targeting the NF-H and M sidearm domain compared with the phosphorylation-independent antibodies (Fig. 4).

Phenotypic Progression of Traumatic Axonal Pathology

The evolution to 2 distinct forms of traumatic axonal pathology was elucidated with NF immunostaining in this study. We found only swelling of axons, with no evidence of axotomy before 6 h post-trauma. Thus, no evidence of primary axotomy (acute disconnection) was observed in this model. Consistent with the well-described progression of post-traumatic axonal pathology, we found discrete bulb formation and disconnection by 24 h postinjury. The typical morphology of these bulbs was 1 roundly swollen region at the terminal ends of disconnected axons. The axonal diameter preceding the bulbs was almost normal demonstrating the discrete nature of this distinct pathology. The diameter of the axon bulbs did not appear to influence disconnection. Large diameter axonal bulbs (up to 50 μ m) and small diameter bulbs (less than 5 μ m) were found to be disconnected. Up to 10 days postinjury, we also observed nondisconnected axonal swellings with large and multiple varicosities along lengths that encompassed several hundred microns of the axon. This morphology appeared very

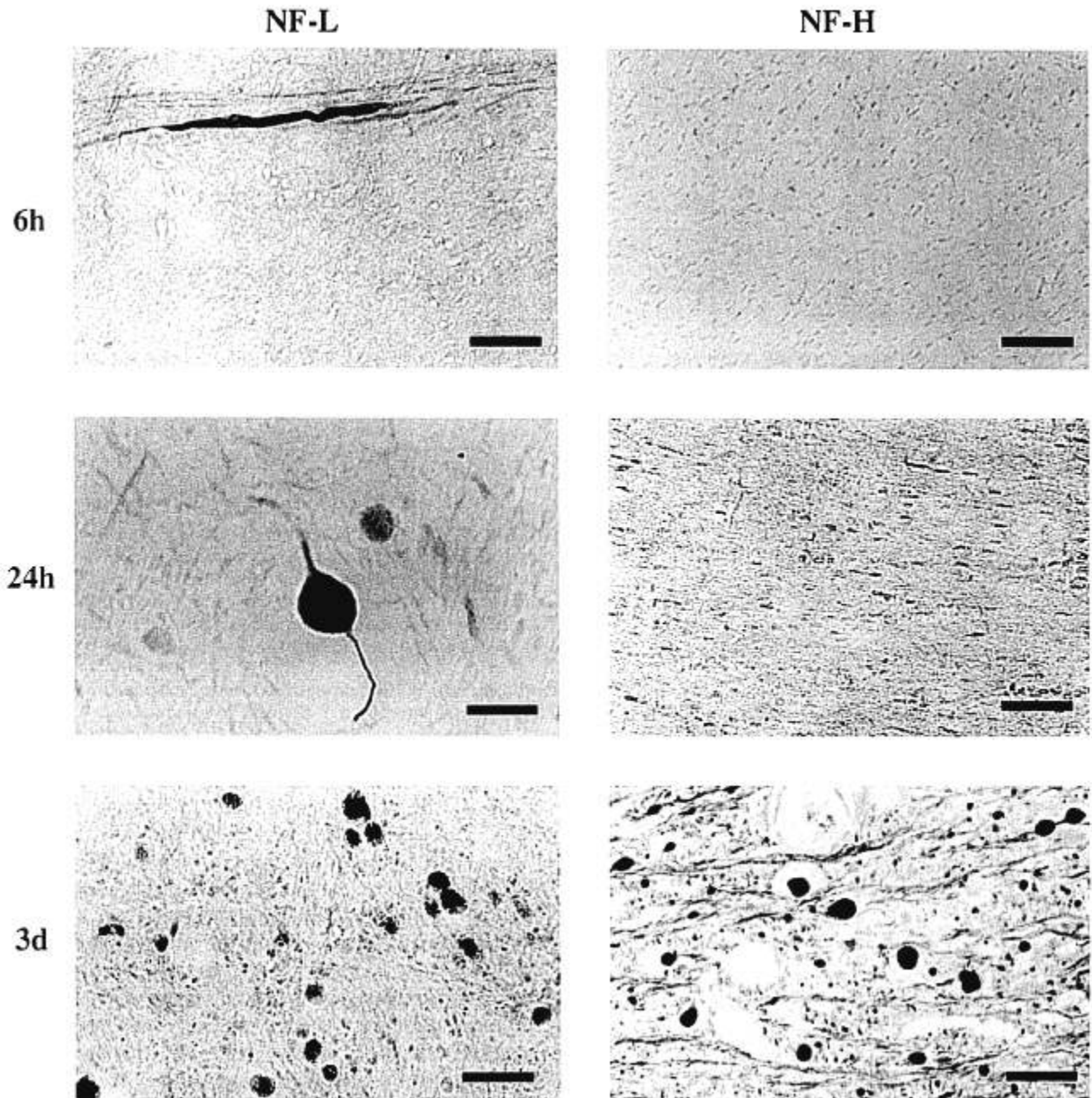


Fig. 2. Representative photomicrographs of NF-L and NF-H immunoreactivity in damaged axons in the subcortical white matter and basal ganglia. Panels to the left demonstrate immunoreactivity of NF-L in swollen axons as early as 6 h postinjury (top), the elucidation of a large swollen bulb formations with axotomy at 24 h postinjury (middle), and a high density of axonal pathology injury detected by the antibody to NF-L at 3 days (d) postinjury (bottom). Panels on the right demonstrate virtually no NF-H immunoreactivity in regions of axonal injury until 3 days postinjury. Bar: 6 h = 180 μ m, 24 h = 20 μ m, 3 d = 40 μ m.

distinct from the individual bulbs affecting only 1 local area of the axon. Therefore, we observed at least 2 phenotypes of matured traumatic axonal pathology, including 1) varicose swellings spread along great lengths of axons, and 2) discrete axonal bulbs found only at the terminal end of disconnected axons.

We also found a regional predilection for specific axonal pathology phenotypes. Regions in which axonal

swellings comprised the only axonal pathology phenotype included long-tract systems of subcortical and deep white matter, while axonal bulbs were more commonly found at anatomic boundaries such as the gray-white matter interface and along margins of ventricles in addition to the basal ganglia and brainstem. However, many white matter regions demonstrated a mixture of varicose swellings and bulbs (Fig. 5).

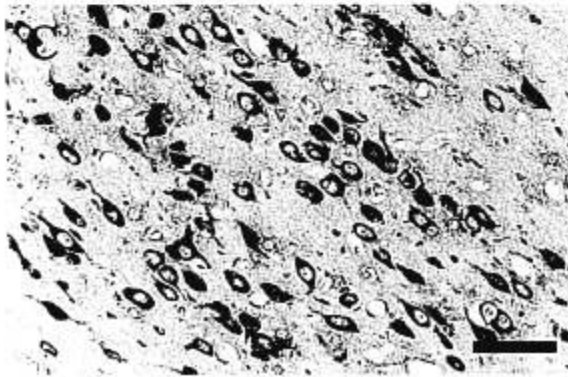
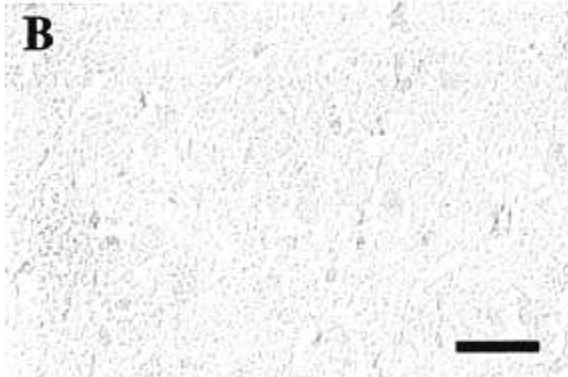
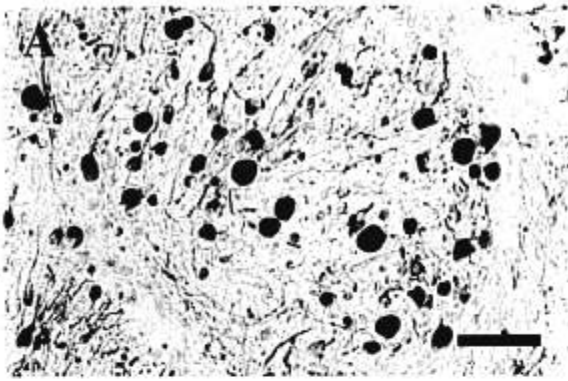


Fig. 3. Representative photomicrographs of NF-M rod and sidearm accumulation in damaged axons. Antibody to NF-M sidearm domain strongly stains damaged axons (A). Antibody to NF-M rod domain does not elucidate axonal injury (B), but does stain neuronal somata as a positive control (C). Bar = 40 μ m.

DISCUSSION

In this study we found several unique features in the development of axonal pathology following diffuse brain injury in the pig: 1) accumulation of NF-L in damaged axons appears much earlier than NF-M and H; 2) accumulation of the sidearm domain, but not the core region of NF-M and H could be identified in damaged axons; 3) both dephosphorylated and phosphorylated NF sidearms were found in damaged axons; and 4) axonal bulbs

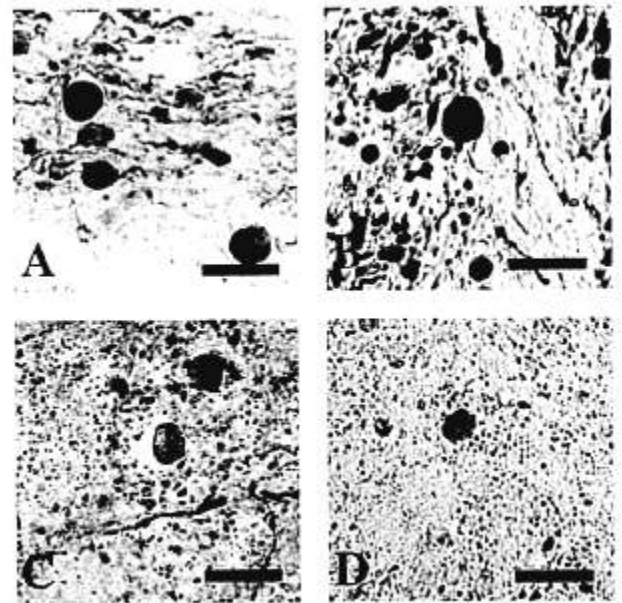


Fig. 4. Representative photomicrographs of axonal pathology in the basal ganglia. Axon damage is darkly stained with antibodies against phosphorylation-independent NF-M and H sidearm domains (A and B) and more lightly, but distinctly, stained with antibodies specific for phosphorylated NF-M and H sidearm domains (C and D). Bar = 40 μ m.

and varicose swellings may represent 2 distinct phenotypes of axonal pathology.

Consistent with previous studies on brain trauma in humans and large animals (5, 9, 20), immunoreactivity of NF-L in axonal swelling was observed in the present study as early as 6 h postinjury. It has been previously suggested that NF-L is more easily identified due to more sensitive immunostaining, or that it more selectively accumulates compared with NF-M and H following trauma (20, 21). However, we found excellent staining identifying NF-M and H accumulation in damaged pig axons by 3 days postinjury, but only modest staining for these particular NFs was observed at 24 h postinjury, and no staining at 6 h postinjury. These data demonstrate there is substantial accumulation of all NF subtypes in damaged axons, but that accumulation of NF-M and H is delayed compared with NF-L. This may suggest possible temporal sequence of cytoskeletal disruption following axonal injury. Immediately following trauma, core NF-68 protein may be a primary target for detachment from the neurofilamentous cytoskeleton. Alternatively, as previously suggested, trauma may accelerate normally occurring NF-L disassembly and migration from a stable neurofilament pool to soluble pool within the axoplasm (20, 22, 23). A curious consideration of selective NF-L disassembly following trauma is that NF-L is a primary constituent of the core of the neurofilament structure, suggesting that it is a more remote target for degradation than NF-M and H, which are found in the exterior circumference of neurofilaments.

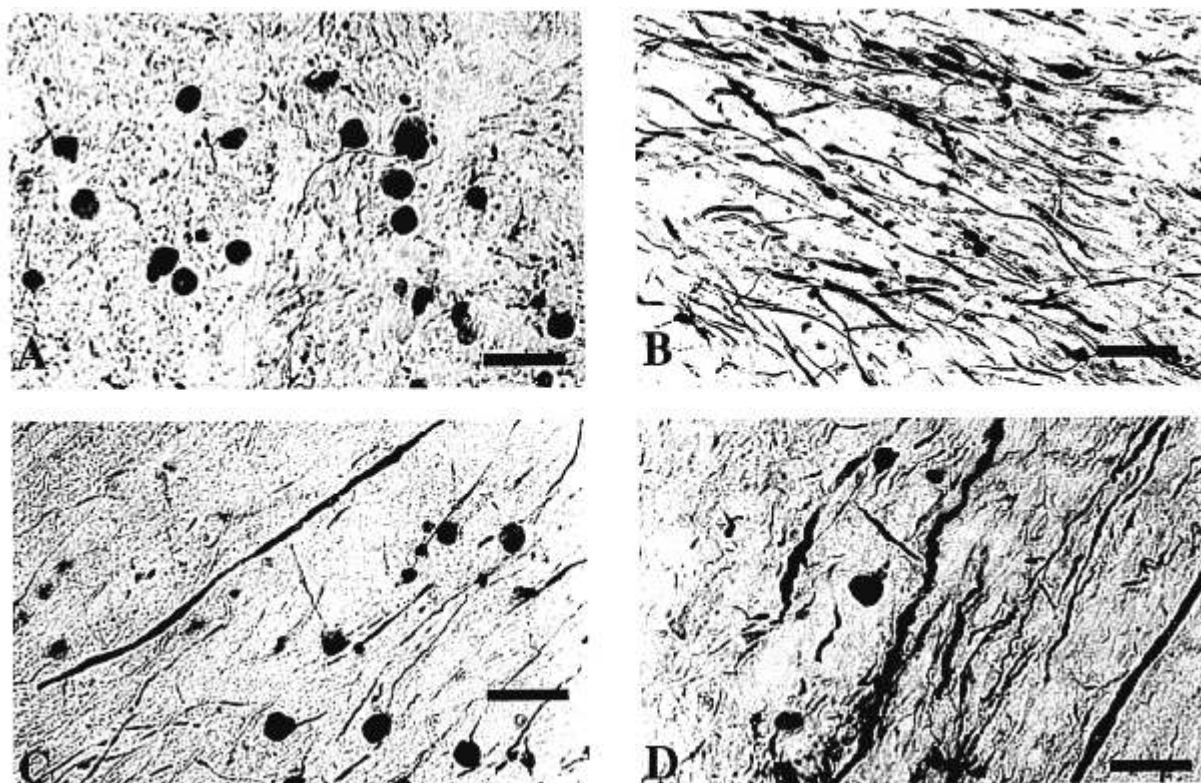


Fig. 5. Representative photomicrographs of NF immunostained sections demonstrating phenotypes of axonal injury at 7 days post-trauma. A high density of isolated axonal bulbs in subcortical white matter demonstrating only 1 localized region of damage in each affected axon (A), a predominance of varicose swellings encompassing long portions of damaged axons in the basal ganglia (B), and a mixture of axonal bulbs and varicose swellings in the white matter at the root of a parietal lobe gyrus (C and D). Bar: 80 μ m for A, 40 μ m for B, C and D.

While the slow axonal transport protein, NF-L, accumulates in damaged axons relatively early following trauma, it is preceded by proteins conveyed via fast axonal transport. Most notably, the fast axonal transport protein, β -amyloid precursor protein (β -APP), has been found accumulating in damaged regions of axons as early as 30 min following brain trauma (24–26). Accordingly, immunostaining for β -APP is now routinely used to elucidate axonal injury at acute postinjury timepoints (26–28). However, β -APP staining only discerns morphologic changes in the axon, while staining for subtypes of NF proteins may reveal specific changes in the axonal cytoskeleton, as suggested by the results in the present study.

In the present study, only antibodies specific for the sidearm domains of NF-M and H stained regions of axonal swellings and bulbs. Antibodies specific to the NF rod domains failed to elucidate axonal pathology at any timepoint, but did demonstrate normal staining of neuronal perikarya as previously characterized (18, 29). Povlishock and colleagues previously used the same set of rod and sidearm-specific antibodies in another animal model of brain trauma and found evidence that the NF sidearms are cleaved post-trauma, leaving the rod domains exposed, yet apparently still intact as part of the

axon cytoskeleton (14). Using the same set of antibodies for Western blot analysis, Hall and colleagues demonstrated cleavage of NF sidearms following axonal transection in the lamprey (18). Accordingly, inertial brain injury in the pig may also induce cleavage of the NF sidearms that accumulate in regions of impaired transport in a delayed fashion compared with accumulation of NF-L. In addition, our results suggest that NF-M and H rod domains may not be primary targets for disassembly following trauma.

The proposed mechanisms underlying NF sidearm changes in axonal injury have focused on elevated intraxonal levels of calcium, activation of μ m calpain, subsequent proteolysis of the NF sidearm (15, 30), and a change in the NF phosphorylation state postinjury (31–35). There is also some evidence that NF dephosphorylation leads rapidly to proteolysis of the sidearms (14, 15, 18, 36). NF-M and H in the stationary axonal cytoskeleton are highly phosphorylated in the multi-phosphorylated region of the sidearm domain (31, 37, 38). In contrast, transported forms of NF are mainly nonphosphorylated (39–41) and it has been suggested that accumulating NF in damaged axons is nonphosphorylated (31, 32, 40). In the present study, we found a high density of bulbs and

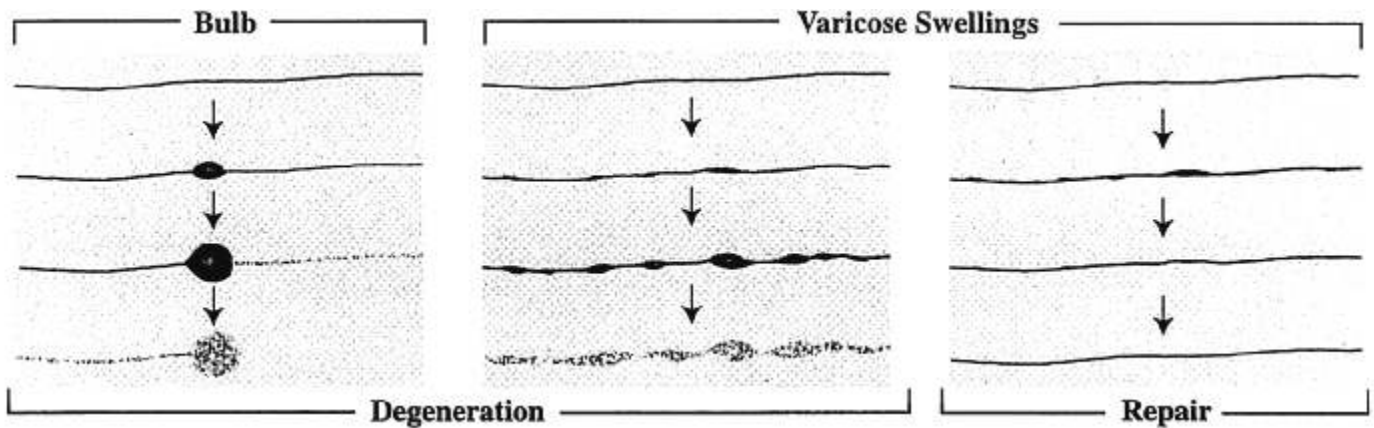


Fig. 6. Schematic illustration demonstrating 3 proposed sequelae of traumatic axonal damage. Localized axonal damage due to nonuniform strain results in catastrophic failure of a discrete region of the cytoskeleton with subsequent bulb formation, disconnection, and degeneration (A). Uniform strain along the axon results in distributed cytoskeletal damage with the development of multiple regions of varicose swellings, and ultimately, degeneration (B). Strain to the axons result in cytoskeletal damage and swelling that are reversed by repair mechanisms (C).

axonal swellings in damaged axons labeled by antibodies specific for phosphorylation-independent NF-M and H sidearm domains and dephosphorylated NF-H sidearm domains at 3 to 10 days post-trauma. To a much lesser extent, we also found phosphorylated NF-M and H sidearm domains in reactive axonal changes, identified with specific antibodies. These findings suggest that while the accumulating NF is predominantly dephosphorylated, some of the sidearms in axonal pathology remain phosphorylated. While these findings may be novel, we cannot presently ascertain whether the phosphorylated sidearms found in axonal pathology are part of an intact cytoskeleton, or if they represent proteolyzed debris that remains phosphorylated.

In this study, we found only axonal swellings at 6 h post-trauma, but by 24 h post-trauma we observed large axonal bulbs. This suggests that there is little to no primary axotomy in this model of diffuse brain injury in the pig, and that the temporal progression to axonal disconnection in pigs is similar to humans, as previously suggested (5, 20). This observation may appear to support the widely accepted premise that axonal pathology proceeds in a stepwise fashion from cytoskeletal disruption to a swelling that progresses into terminal bulb formation following axotomy (19, 42). However, we have previously suggested that there may be more than 1 pathway in the development of post-traumatic axonal pathology. While it seems clear that some axonal swellings develop into axonal bulbs, certain types of axonal swellings may represent a distinct phenotype of matured axonal pathology. At all timepoints, from 24 h up to 10 days postinjury, both axonal bulbs and swellings could be identified. However, major distinctions in the morphology and distribution between axonal swellings and bulbs were

noted. Axonal swellings were often elongated with a tortuous orientation in combination with multiple varicosities in segments ranging from 70–300 μm in length. In contrast, axonal bulbs were typically found to display only 1 discrete round distention at the terminal stump, preceded by a remarkably normal axon diameter. Regions in which axonal swellings comprised the only axonal pathology phenotype included long-tract systems of subcortical and deep white matter. In comparison, axonal bulbs were more commonly found at anatomic boundaries such as the gray-white matter interface and along margins of ventricles in addition to the basal ganglia and brainstem. We propose that varying loading conditions during injury assumed by axons traversing different planes might affect the subsequent pathologic phenotype. With a uniform strain such as tensile elongation distributed along the axon, great lengths may be damaged leading to elongated swellings and disorientation. On the other hand, nonuniform strain, which may occur at anatomic boundaries, may affect 1 discrete region of the axon. This discrete damage may then lead to localized catastrophic failure of the cytoskeleton with resultant disconnection and bulb formation without remarkable damage in more proximal regions.

Based on our results, disconnection of axons appears more related to the mechanical loading conditions at the time of injury (e.g. tensile vs shear strain) rather than the extent of swelling. For example, disconnection was not a typical feature of axonal swellings even though some reached diameters of greater than 40 μm . Alternatively, disconnection was commonly observed in association with axonal bulbs of only a few μm in diameter. Therefore, we may have to revise current hypotheses of the temporal course of axon degeneration. While Wallerian

degeneration of axonal bulbs is well established, the fate of axonal swellings remains unclear. It is possible that many swollen axons may actually undergo repair, as schematically illustrated in Figure 6. As has previously been reported, axons injured close to their cell of origin and proximal to their collaterals are most likely to undergo degenerative changes, whereas axons injured far from their cell of origin and distal to their collateral branches may survive (43, 44). Accordingly, axonal swellings found in long tracts may be less likely to degenerate than axonal bulbs located at anatomic boundaries.

Taken together, these findings suggest that there is a specific temporal course in NF disassembly, dephosphorylation, and accumulation in axons following brain trauma. The character and rate of these changes appears to be dependent on the NF subtype. Furthermore, the evolution of these changes may occur in isolated regions of axons or be distributed along great lengths of axons possibly reflecting local mechanical loading conditions at the time of injury.

ACKNOWLEDGMENTS

We would like to thank Drs. Virginia Lee and John Trojanowski for the generous gift of antibodies and Jeanne Marks for her excellent preparation of this manuscript.

REFERENCES

- Gennarelli TA. Head injury in man and experimental animals: Clinical aspects. *Acta Neurochir (Suppl)* 1983;32:1-13
- Graham DI, McLellan D, Adams JH, et al. The neuropathology of severe disability after head injury. *Acta Neurochir (Suppl)* 1983;32:65-7
- Adams JH, Graham DI, Gennarelli TA. Head injury in man and experimental animals. *Acta Neurochir (Suppl) (Wien)* 1983;32:15-30
- Vanezis P, Chan KK, Scholtz CT. White matter damage following acute head injury. *Forensic Sci Int* 1987;35:1-10
- Grady MS, McLaughlin MR, Christman CW, Valadka AB, Fligner CL, Povlishock JT. The use of antibodies targeted against the neurofilament subunits for the detection of diffuse axonal injury in humans. *J Neuropathol Exp Neurol* 1993;52:143-52
- Pettus EH, Christman CW, Gielbel ML, Povlishock JT. Traumatically induced altered membrane permeability. *J Neurotrauma* 1994;11:507-22
- Pettus EH, Povlishock JT. Characterization of a distinct set of intraxonal ultrastructural changes associated with traumatically induced alteration in axolemmal permeability. *Brain Res* 1996;722:1-11
- Povlishock JT, Christman CW. Diffuse axonal injury. In: Waxman SG, Kocsis JD, Stys PK, eds. *The axon: Structure, function and pathophysiology*. New York: Oxford University Press, 1995:504-29
- Povlishock JT, Gielbel ML, Pettus EH. Traumatically induced alterations in axolemma permeability are associated with a distinct subset of intra-axonal cytoskeletal changes. *J Neurotrauma* 1995;12:417
- Povlishock JT, Pettus EH. Traumatically induced axonal damage: Evidence for enduring changes in axolemma permeability with associated cytoskeletal change. *Acta Neurochir* 1996;66:81-6
- Hisanaga S, Hirokawa N. Molecular architecture of the neurofilament II. Reassembly process of neurofilament L protein in vitro. *J Mol Biol* 1990;211:871-82
- Carden MJ, Trojanowski JQ, Schlaepfer WW, Lee V. Two-stage expression of neurofilament polypeptides during rat neurogenesis with early establishment of adult phosphorylation patterns. *J Neurosci* 1987;7:3489-504
- Lee VMY, Otvos L, Jr., Carden MJ, Hollosi M, Dietzschold B, Lazzarini RA. Identification of the major multiphosphorylation site in mammalian neurofilaments. *Proc Natl Acad Sci USA* 1988;85:1998-2002
- Povlishock JT, Marmarou A, McIntosh TK, Trojanowski JQ, Mori J. Impact acceleration injury in the rat: Evidence for focal axolemmal change and related neurofilament sidearm alteration. *J Neuropathol Exp Neurol* 1997;56:347-59
- Maxwell WL, Povlishock JT, Graham DI. A mechanistic analysis of nondisruptive axonal injury: A review. *J Neurotrauma* 1997;14:419-40
- Smith DH, Chen X-H, Xu B-N, McIntosh TK, Gennarelli TA, Meaney DF. Characterization of diffuse axonal pathology and selective hippocampal damage following inertial brain trauma in the pig. *J Neuropathol Exp Neurol* 1997;56:822-34
- Schmidt ML, Carden MJ, Lee VMY, Trojanowski JQ. Phosphate-dependent and independent neurofilament epitopes in the axonal swellings of patients with motor neuron disease and controls. *Lab Invest* 1987;56:282-94
- Hall GF, Lee VMY. Neurofilament sidearm proteolysis is a prominent early effect of axotomy in lamprey giant central neurons. *J Comp Neurol* 1995;353:38-49
- Povlishock JT. Traumatically induced axonal injury: Pathogenesis and pathobiological implications. *Brain Pathol* 1992;2:1-12
- Christman CW, Grady SM, Walker SA, Holloway KL, Povlishock JT. Ultrastructural studies of diffuse axonal injury in humans. *J Neurotrauma* 1994;11:173-86
- Christman CW, Salvant JB, Walker SA, Povlishock JT. Characterization of a prolonged regenerative attempt by diffusely injured axons following traumatic brain injury in the adult cat: A light and electron microscopic immunocytochemical study. *Acta Neuropathol (Berl)* 1997;94:329-37
- Angelides KJ, Smith KE, Takeda M. Assembly and exchanges of intermediate filament proteins of neurons: Neurofilaments are dynamic structures. *J Cell Biol* 1989;108:1495-506
- Povlishock JT. Pathobiology of traumatically induced axonal injury in animals and man. *Ann Emerg Med* 1993;22:980-6
- Ohgami T, Kitamoto T, Tateishi J. Alzheimer's amyloid precursor protein accumulates within axonal swellings in human brain lesions. *Neurosci Lett* 1992;136:75-78
- Pierce JES, Trojanowski JQ, Graham DI, Smith DH, McIntosh TK. Immunohistochemical characterization of alterations in the distribution of amyloid precursor proteins and amyloid b peptide following experimental brain injury in the rat. *J Neurosci* 1996;16:1083-90
- Gentleman SM, Nash MJ, Sweeting CJ, et al. b-amyloid precursor protein (b-APP) as a marker for axonal injury after head injury. *Neurosci Lett* 1993;160:134-44
- Sherriff FE, Bridges LR, Sivaloganathan S. Early detection of axonal injury after human head trauma using immunocytochemistry for b-amyloid precursor protein. *Acta Neuropathol* 1994;87:55-62
- Kawarabayashi T, Shoji M, Harigaya Y, Yamaguchi H, Hirai S. Expression of APP in the early stage of brain damage. *Brain Res* 1991;563:334-8
- Pleasure SJ, Selzer ME, Lee VMY. Lamprey neurofilaments combine in one subunit the features of each mammalian NF triplet protein but are highly phosphorylated only in large axons. *J Neurosci* 1989;9:698-709
- Okonkwo DO, Pettus EH, Mori J, Povlishock JT. Alteration of the neurofilament sidearm and its relation to neurofilament compaction occurring with traumatic axonal injury. *Brain Res* 1998;784:1-6

31. Postmantur RM, Hayes RL, Dixon CE, Taft WC. Neurofilament 68 and neurofilament 200 protein levels decrease after traumatic brain injury. *J Neurotrauma* 1994;11:533-44
32. Wang W, Hamberger A, Yang Q, Haglid KG. Changes in neurofilament protein NF-L and NF-H immunoreactivity following kainic acid-induced seizures. *J Neurochem* 1994;62:739-48
33. Fineman I, Hovda DA, Smith M, Yoshino A, Becker DP. Concussive brain injury is associated with a prolonged accumulation of calcium: A ⁴⁵Ca autoradiographic study. *Brain Res* 1993;624:94-102
34. Mata M, Staple J, Fink DJ. Changes in intra-axonal calcium distribution following nerve crush. *J Neurobiol* 1986;17:449-67
35. Mata M, Kupina N, Fink DJ. Phosphorylation-dependent neurofilament epitopes are reduced at the node of Ranvier. *J Neurocytol* 1992;21:199-210
36. Waegh SM, Lee VMY, Brady ST. Local modulation of neurofilament phosphorylation, axonal caliber, and low axonal transport by myelinating Schwann cells. *Cell* 1992;68:451-63
37. Shaw G, Osborn M, Weber K. Reactivity of a panel of neurofilament antibodies on phosphorylated and dephosphorylated neurofilaments. *Eur J Cell Biol* 1986;42:1-9
38. Gotow T, Tanaka J. Phosphorylation of neurofilament H subunit as related to arrangement of neurofilaments. *J Neurosci Res* 1994;37:673
39. Hollenbeck PJ. The transport and assembly of the axonal cytoskeleton. *J Cell Biol* 1989;108:223-7
40. Nixon RA, Sihag GK. Neurofilament phosphorylation: A new look at regulation and function. *Trends Neurosci* 1991;15:501-6
41. Meller D, Bellander BM, Kastner RS, Ingvar M. Immunohistochemical studies with antibodies to neurofilament proteins on axonal damage in experimental focal lesions in the rat. *J Neurol Sci* 1993;117:164-74
42. Jafari SS, Maxwell WL, Neilson M, Graham DI. Axonal cytoskeletal changes after non-disruptive axonal injury. *J Neurocytology* 1997;26:207-21
43. Barron KD. Axon reaction and its relevance to CNS trauma. In: Grossman RG, Gildenberg PL, eds. *Head injuries: Basic and clinical aspects*. New York: Raven Press, 1982:P15
44. Povlishock JT, Becker DP. Fate of reactive axonal swellings induced by head injury. *Lab Invest* 1985;52:540-52

Received October 23, 1998

Revision received February 17, 1999

Accepted February 18, 1999